


Article

# Multi-Physics Ensemble versus Atmosphere–Ocean Coupled Model Simulations for a Tropical-Like Cyclone in the Mediterranean Sea

Antonio Ricchi <sup>1,\*</sup> , Mario Marcello Miglietta <sup>2</sup> , Davide Bonaldo <sup>1</sup>, Guido Cioni <sup>3</sup>,  
Umberto Rizza <sup>2</sup> and Sandro Carniel <sup>1</sup>

<sup>1</sup> Institute of Marine Sciences (ISMAR-CNR), 30121 Venice, Italy; davide.bonaldo@ve.ismar.cnr.it (D.B.); sandro.carniel@ismar.cnr.it (S.C.)

<sup>2</sup> Institute of Atmospheric Sciences and Climate (ISAC-CNR), 73100 Lecce, Italy; m.miglietta@isac.cnr.it (M.M.M.); u.rizza@isac.cnr.it (U.R.)

<sup>3</sup> Max Planck Institute for Meteorology, Bundesstr., 53 D-20146 Hamburg, Germany; guido.cioni@mpimet.mpg.de

\* Correspondence: antonio.ricchi@ve.ismar.cnr.it

Received: 6 March 2019; Accepted: 3 April 2019; Published: 15 April 2019



**Abstract:** Between 19 and 22 January 2014, a baroclinic wave moving eastward from the Atlantic Ocean generated a cut-off low over the Strait of Gibraltar and was responsible for the subsequent intensification of an extra-tropical cyclone. This system exhibited tropical-like features in the following stages of its life cycle and remained active for approximately 80 h, moving along the Mediterranean Sea from west to east, eventually reaching the Adriatic Sea. Two different modeling approaches, which are comparable in terms of computational cost, are analyzed here to represent the cyclone evolution. First, a multi-physics ensemble using different microphysics and turbulence parameterization schemes available in the WRF (weather research and forecasting) model is employed. Second, the COAWST (coupled ocean–atmosphere wave sediment transport modeling system) suite, including WRF as an atmospheric model, ROMS (regional ocean modeling system) as an ocean model, and SWAN (simulating waves in nearshore) as a wave model, is used. The advantage of using a coupled modeling system is evaluated taking into account air–sea interaction processes at growing levels of complexity. First, a high-resolution sea surface temperature (SST) field, updated every 6 h, is used to force a WRF model stand-alone atmospheric simulation. Later, a two-way atmosphere–ocean coupled configuration is employed using COAWST, where SST is updated using consistent sea surface fluxes in the atmospheric and ocean models. Results show that a 1D ocean model is able to reproduce the evolution of the cyclone rather well, given a high-resolution initial SST field produced by ROMS after a long spin-up time. Additionally, coupled simulations reproduce more accurate (less intense) sea surface heat fluxes and a cyclone track and intensity, compared with a multi-physics ensemble of standalone atmospheric simulations.

**Keywords:** tropical-like cyclones; coupled model; sensitivity; Multi-Physics Ensemble; PBL; WRF; SWAN; ROMS; COAWST

## 1. Introduction

The Mediterranean basin is one of the most cyclogenetic areas in the world, with an average of one hundred pressure lows every year [1]. Extra-tropical depressions, typical of this area, are often caused by the interaction of upper level disturbances with low-level baroclinicity, sometimes favored by the complex morphology of the basin, as in the case of so-called Genoa low [2]. Such cyclones can be particularly intense and associated with heavy precipitation events (HPEs) and severe wind gusts.

Occasionally, some Mediterranean cyclones may exhibit tropical-like features in their mature stage, such as a barotropic structure, the presence of a warm core in the center of the storm with structured and spiral convection around it, and sustained winds over 100 km/h [3–9]. Due to their resemblance to tropical cyclones, they are usually called “medicanes” (MEDiterranean hurriCANES; [10]) or MTLCs (Mediterranean tropical-like cyclones, [11]). Several studies have demonstrated that these systems, which usually originate from a baroclinic wave, can transition into barotropic structures when certain environmental conditions are met [12].

Due to the evolution of NWP (numerical weather prediction) models, it has become possible to study these phenomena in detail by simulating their fine horizontal and vertical structure, a feature that is hardly resolved by satellite or in-situ observations, also considering these cyclones spend most of their lifetime over the sea. However, despite the scientific efforts emerging in a variety of sensitivity studies, even now NWP models suffer from a significant forecast skill reduction in the simulation of MTLCs, as they sometimes intensify the cyclone in an unrealistic way, or fail to foresee its development and evolution accurately. This predictability limitation depends on many factors and varies from case to case [13]. In some events, a large sensitivity to the location of the model domain and to the horizontal grid resolution [14] is observed, while in other cases parameterization schemes play a fundamental role [15–17].

Other studies (e.g., [15,18]) have shown that the large scale forcing at the initial time is the main factor of uncertainty in the numerical simulations of medicanes.

Generally, an important role is also played by the lateral and lower boundaries, such as the SST field [19,20] the accuracy of which is fundamental for a realistic simulation of these cyclones [16]. Thus, coupled ocean–atmosphere modeling systems have generally emerged as useful in order to improve the simulation skill [21,22] via a better representation of the air–sea interaction processes.

Some of these studies have analyzed independently the ability of a multi-physics ensemble and of a coupled atmosphere–ocean model to simulate MTLCs; however, none have studied the two implementations comparatively, in order to identify which one is more beneficial in terms of model skill. This point is important for an operational center, considering that computational resources are not infinite. For this reason, in this study, we investigate which one of the two approaches is better suited to reproduce the evolution of an MTLC. As a case study, we choose the MTLC that occurred in January 2014 [6]. Since this system spent most of its life cycle over the sea, it represents an ideal case to assess the effects of air–sea interactions. In this effort, simulations with a growing level of complexity in the representation of the SST field are considered here, also in order to better understand its influence on the model simulations.

The MTLC developed in the early morning of 19 January 2014 in the Alboran Sea due to a baroclinic wave extending from the Atlantic to the Mediterranean. In the following hours, the cyclone deepened down to a pressure minimum of 990 hPa, causing sustained wind speeds up to 100 km/h recorded in Gibraltar airport [6]. Between the morning of 19 January 2014 and the late afternoon of 20 January 2014, the system moved across the Western Mediterranean, eventually making landfall near Napoli (Southern Italy) at around 16 UTC. The cyclone then moved northward for about 300 km, crossing the Apennines mountain range, and intensified again after reaching the Adriatic Sea. In the following hours, its track rotated counterclockwise, approaching the Italian coasts; in this phase, the cyclone intensified very rapidly, showing tropical-like features once again [6]; finally, it vanished over the coasts of Albania (Figure 1).

In the first group of simulations, we employed a multi-physics ensemble implementing different microphysics and boundary layer schemes. For the setup that produces the most realistic simulation, we modified the SST dataset, in order to evaluate the effect of a finer horizontal resolution; we also used a uniform SST over the whole domain (using the average value), with the aim of evaluating the effect of SST gradients. The second group of simulations was performed with the coupled atmosphere–ocean modeling system, analyzing also the effect of the coupling timestep. Finally, an analysis of the computational resources required for these two types of runs was performed.

In Section 2, the numerical approach and the COAWST model are described in detail. Results are discussed in Section 3; conclusions are drawn in Section 4.

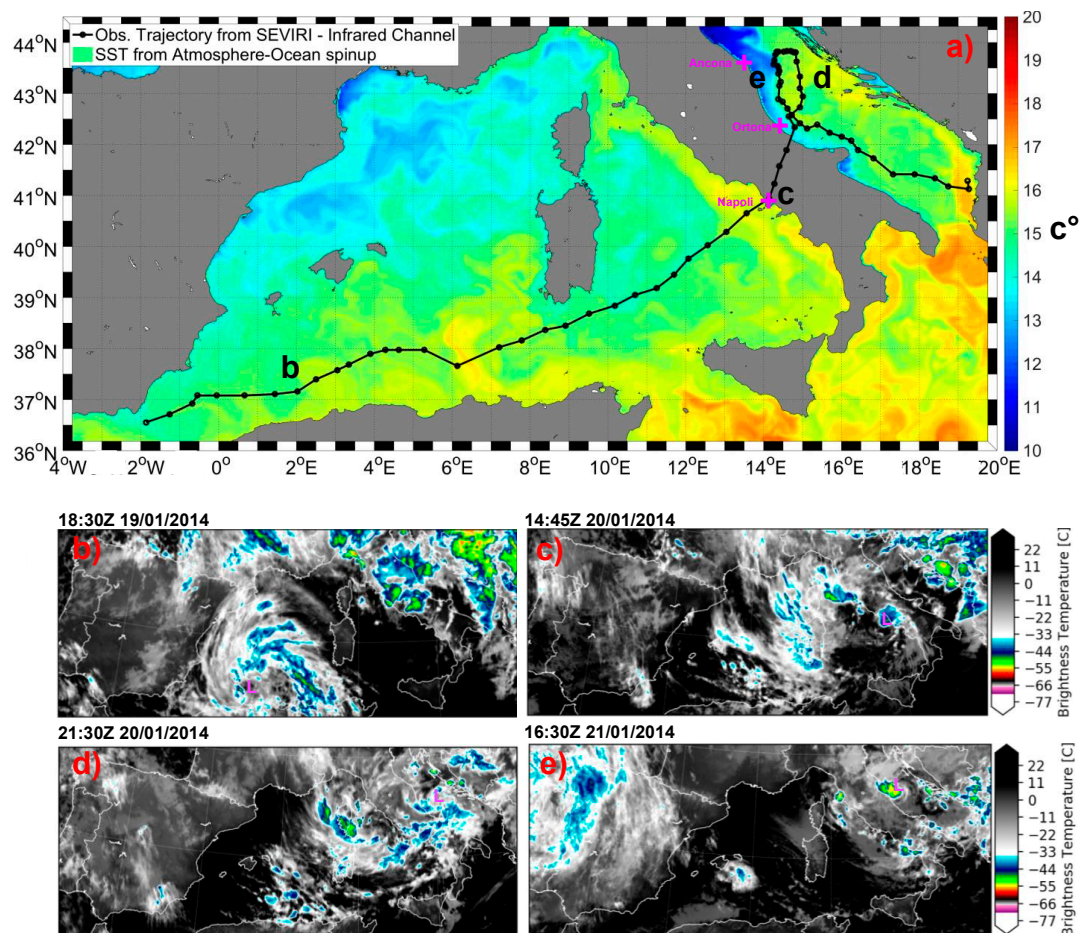


**Figure 1.** Observed trajectory (a) and satellite infrared imagery at different times (b–e). The cyclone trajectory was derived using 5 min rapid-scan infrared SEVIRI satellite imagery by manually identifying the position of the cyclone.

## 2. Methods

### 2.1. COAWST Model

The COAWST model (coupled ocean–atmosphere wave sediment transport; [22–26]) is a numerical framework that entails various coupling methods among the atmospheric model WRF (weather research and forecasting; [27]), the oceanic model ROMS (regional ocean modeling system; [28]), and the sediment model CSTM (community sediment transport model; [29]). In the latest version, COAWST also offers the possibility of choosing between the WWIII model (wave watch 3) and the SWAN model (simulating waves in nearshore) to simulate the evolution of surface waves. The coupling among the models is obtained through the exchange of prognostic fields and is managed by the MCT libraries (model coupling toolkit; [24,30,31]). In detail, in the implementation used in this work, the WRF model provided (Figure 2) the ROMS model with the heat and the momentum fluxes and then received SST fields. Thus, in the coupled configuration, the ROMS model did not calculate the heat fluxes again, but used those provided by the WRF model in order to guarantee the full consistency between the two models.

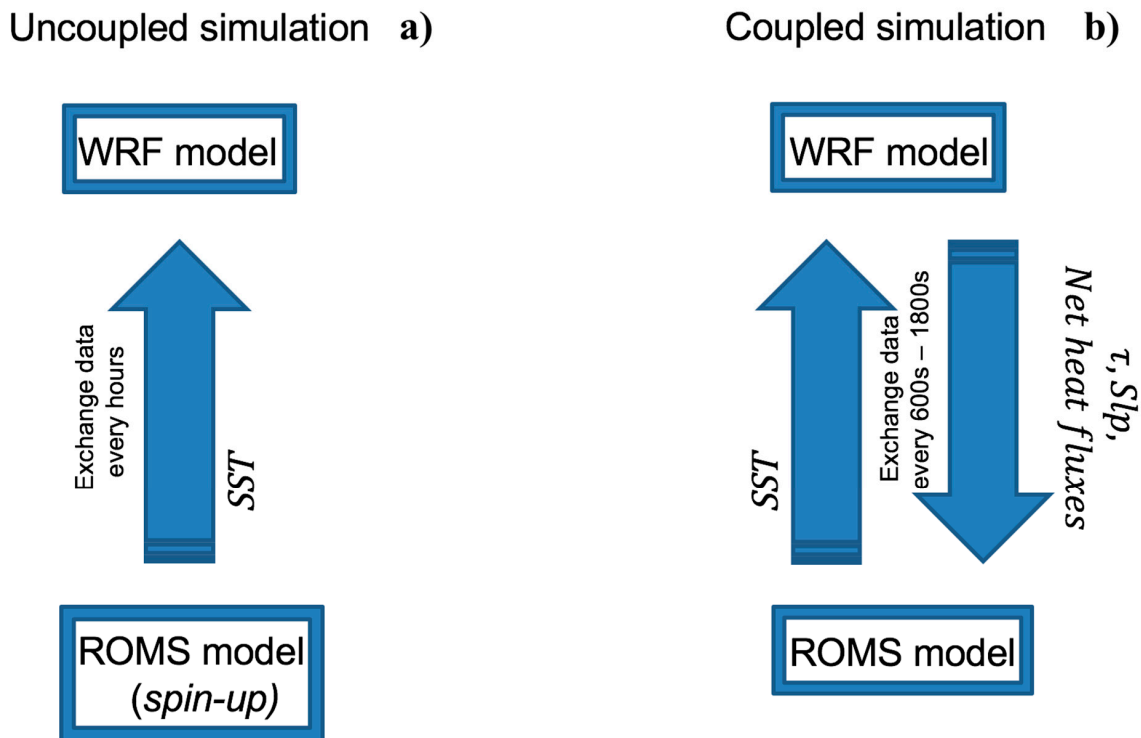


**Figure 2.** Sketch of different model configurations: (a) uncoupled approach where the sea surface temperature (SST), updated every hour, is used as a lower boundary in the WRF (weather research and forecasting) model; (b) coupled approach with ocean and atmosphere models exchanging energy and momentum fluxes (data exchange may occur at different intervals, i.e., every 600 s and 1800 s).

The COAWST model allows the coupling of the models either on the same grid or on different ones. As shown in Figure 3, the WRF domain configuration used in this work is based on three grids one-way nested into each other (Figure 3), characterized by 27 km (D01), 9 km (D02), and 3 km (D03) horizontal spacing. The inner domain has  $925 \times 563$  horizontal grid points, with 60 vertical levels, with deep convection explicitly resolved. The first vertical level is at the height of 12 m above the ground. The microphysics scheme in the coupled runs was WDM5 (WRF Double-Moment 5-class scheme), based [32], while, in order to parameterize the planetary boundary layer (PBL), the approach of [33] was used. As a shortwave radiation scheme, we used RRTMG (Rapid Radiative Transfer Model; [34]), and for the longwave we used methods used by [35]. In D01 and D02, the Kain-Fritsch (KF) cumulus parameterization was used. Following [6], the simulation was initialized at 00UTC, 19 January 2014, using the GFS-FNL (GFS final reanalysis) dataset as initial/boundary conditions for D01. The simulation in D03 was forced with the output fields in D02 with an hourly frequency; the integration timestep was 15 s. The topography had a resolution of 30", with land-surface parameters taken from the MODIS dataset.

As demonstrated in [6], the SST lower boundary field is critical for the simulation of cyclone intensity and trajectory. Therefore, we decided to use the SST fields generated by a coupled run after a long spin-up. Atmospheric simulations were forced with boundary and initial conditions taken from the same dataset used for the "final" simulation (GFS-FNL). Two-way coupled atmospheric-ocean runs were performed for 35 days, restarting the simulations every 72 h. After the latter period, the atmospheric model started from the reanalyses at that time, in order to remove possible divergence of the model simulations with respect to the reanalyses, while the ocean model took the initial condition from the previous run output. Ocean boundary conditions were taken from the MFS [36] reanalysis datasets (see Section 4). The ocean model domain was similar to that employed for the atmospheric model, with a grid spacing of 3 km (Figure 3). The vertical discretization consisted of 30 vertical levels

with increased resolution near the surface, in order to better describe the ocean mixed layer (OML) and used a bathymetry generated by the GEBCO dataset, characterized by a 30'' resolution [37]. As a mixing scheme, we used the GLS (generic length scale; [38]) approach. The ocean model initialization was obtained from the coupled atmosphere–ocean spin-up described in Section 2.4. In this application we did not use river input and sediment interaction with water masses.

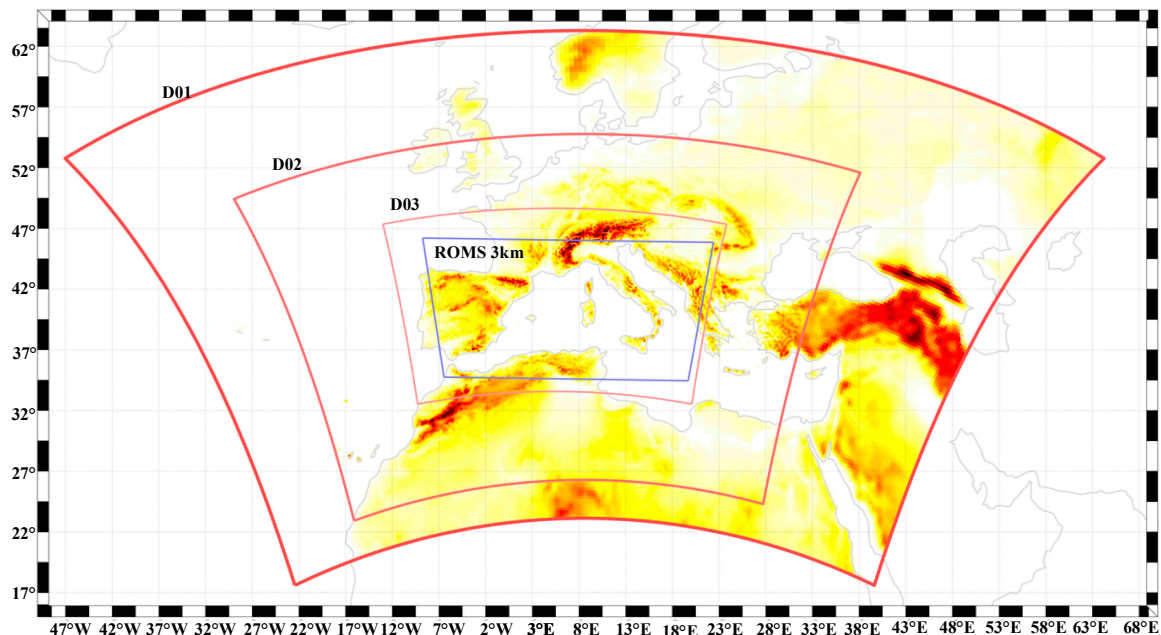


**Figure 3.** Topography and domain configuration used for the coupled and uncoupled simulations. Red lines highlight the WRF domains and the grey box delimits the ROMS model.

## 2.2. Experimental Design

The main purpose of this work is to compare different numerical approaches for the simulation of an MTLC. In particular, we compare a multi-physics ensemble uncoupled approach (WRFUNC) with a coupled modeling implementation, using different coupling times (AO) (Figure 2). The comparison is carried out in terms of cyclone trajectory, intensity, and timing. All the performed simulations are summarized in Table 1. For the uncoupled simulations, we performed a comprehensive study using different microphysics and PBL schemes, which, as discussed in [15], may affect both the cyclone track and intensity. Eighteen runs, which differ for the microphysics scheme, the PBL scheme, and the type of SST used, were performed. The configuration that showed the best results is used for comparison with the coupled model simulations (Figure 2), in order to identify the best strategy for operational use, considering that the two implementations (multi-physics ensemble versus coupled modeling system) have a similar computational burden.

## 2.3. Uncoupled Simulations (WRFUNCP1-15)

The numerical setup of the control run WRFUNC-CTL (Table 1) is based on the results of [6,15]. Thus, the Thompson scheme for the parametrization of microphysics [39] and the Mellor–Yamada–Janjic parametrization scheme for the PBL [40] were used. Additionally, a high-resolution SST field, extrapolated with hourly frequency from a ROMS model run (see next section), was used. In the domains D01 and D02 (Figure 3), which were not covered by the ROMS domain, we used the SST fields taken from the CMEMS dataset “Copernicus” [36], with a horizontal resolution of 6 km.

**Table 1.** List of model experiments reporting the microphysical scheme (MP), the planetary boundary layer (PBL) scheme, and the sea surface temperature (SST) approach.

Runs	MP	MP	PBL	PBL	SST
WRFUNCP-CTL	8	Thompson	2	MYJ	3 km Spinup
WRFUNCP-1	1	Kessler	2	MYJ	3 km Spinup
WRFUNCP-2	2	Lin	2	MYJ	3 km Spinup
WRFUNCP-3	3	WSM3	2	MYJ	3 km Spinup
WRFUNCP-4	4	WSM5	2	MYJ	3 km Spinup
WRFUNCP-5	5	<i>Eta (Ferrier)</i>	2	MYJ	3 km Spinup
WRFUNCP-6	6	WSM6	2	MYJ	3 km Spinup
WRFUNCP-7	14	WDM5	2	MYJ	3 km Spinup
WRFUNCP-8	16	WDM6	2	MYJ	3 km Spinup
WRFUNCP-9	14	WDM5	1	YSU	3 km Spinup
WRFUNCP-10	14	WDM5	2	MYJ	3 km Spinup
WRFUNCP-11	14	WDM5	4	QNSE	3 km Spinup
WRFUNCP-12	14	WDM5	5	MYNN2	3 km Spinup
WRFUNCP-13	14	WDM5	8	<i>BouLac</i>	3 km Spinup
WRFUNCP-14	14	WDM5	2	MYJ	OML-1D
WRFUNCP-15	14	WDM5	2	MYJ	FLAT-SST
AO1	14	WDM5	2	MYJ	AO-1800s
AO2	14	WDM5	2	MYJ	AO-600s

In every uncoupled run, a slab ocean model [41] was employed, so that the initial value of SST changed with time according to the heat fluxes, taking into account the depth of the mixed layer (50 m in these simulations) and the lapse rate (set equal to 0.14 °C/m). This approach, combined with the use of a high-resolution initial SST, allowed us to update the SST in a way similar to the coupled runs. Starting from this configuration, we changed the microphysics scheme as shown in Table 1 (WRFUNC1-8), and, for the best microphysics (WDM5), we used different PBL schemes (WRFUNC-9-13). In order to test the effect of the mixed layer depth (MLD), we changed its value from 50 to 80 m (WRFUNC-14). Finally, to better understand the influence of the gradients of SST in the Mediterranean on the MTLT, another simulation was performed (WRFUNC-15) using in D03 the average SST along the MTLT trajectory, without changing the SST field in the D01-D02 domains.

#### 2.4. Coupled Simulations (AO1-2)

Coupled simulations used a two-way nesting configuration of WRF and ROMS models. Starting from the configuration WRFUNC-10, which shows the best performance among the uncoupled runs, two coupled simulations (AO1-2) were performed, and they used respectively 1800 and 600 s as exchange times (of SST and surface fluxes) between the ocean and the atmosphere.

#### 2.5. Ocean Spin-Up

A long spin-up time of the oceanic model is crucial in order to reach stability in the oceanic fields on the fine numerical grid. In order to achieve this goal, a simulation was performed over 35 days. As discussed earlier, WRF and ROMS are two-way nested. The oceanic field at 00UTC on 19 January 2014, at the end of the spin-up time, was used to force both the uncoupled atmospheric model simulations (only the SST) and the coupled model (3D oceanic fields) runs.

## 2.6. Data

The analyzed event was characterized by a particularly long evolution and by a prolonged track over the Western Mediterranean basin. With the purpose to investigate the physical characteristics of this MTLC, we used an infrared satellite dataset. In particular, the trajectory of the cyclone was identified using the SEVIRI data (EUMETSAT), with a frequency of 15 min. Since the MTLC moves mostly over the open sea, the only surface data available in the central phase of its lifetime are those over the Italian territory. We analyze sea level pressure and wind speed in the following section. The surface stations considered here are Napoli (where the cyclone made its first landfall), Ortona, and Ancona (both close to the track of the cyclone in the Adriatic Sea).

## 3. Results

In this section, we describe the results of the multi-physics ensemble and the coupled model simulations. First, the impact of various physical schemes and SST implementations on the MTLC is analyzed. Next, the results of the coupled model configuration for different communication time intervals and the comparison with the ensemble multi-physics are presented. In particular, in order to compare the trajectory of the simulated MTLC with the observed track (Figure 1), the values of the minimum pressure are saved together with the maximum wind intensity within a radius of 200 km from the cyclone center. In order to quantify the distance between the simulated and the observed trajectory, we consider purely geometrical distance (that is, independent of time) at each point of the observed track. Lastly, we estimate the multi-physics ensemble approach compared to coupled runs in terms of computational resources.

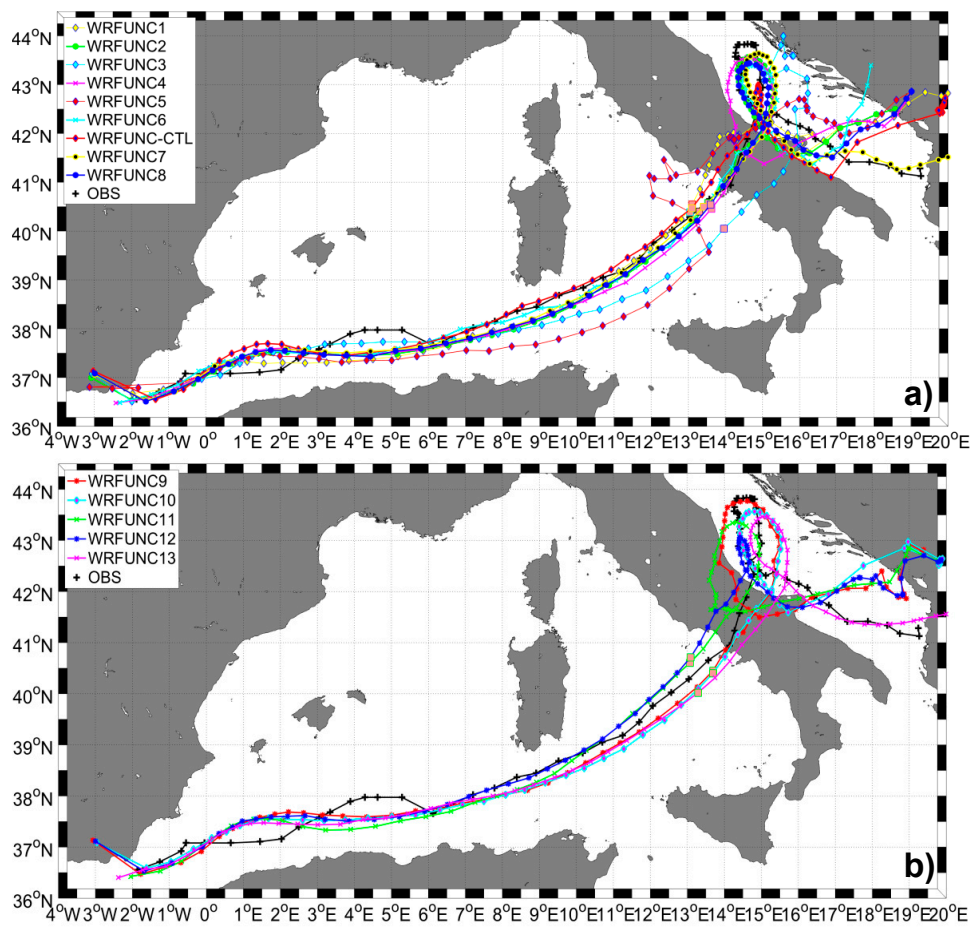
### 3.1. Microphysics Schemes

Figure 4a shows that changes in the microphysics parametrization may affect the trajectories of the MTLC. During its evolution, it is evident that WRFUNC1, WRFUNC3, and WRFUNC5 describe a path of the cyclone significantly different from the observed trajectory. In particular, regarding when the MTLC moved over the Sardinia Channel, the trajectories in WRFUNC3 and WRFUNC5 diverge compared to the observed track, remaining on its southern side for most of the transit over the Tyrrhenian Sea. After the landfall at around 17:00 UTC, 20 January 2018 (Figure 5a), the weakening of the cyclone made identification of the pressure minimum difficult (two weak lows can be distinguished: one over the Southern Tyrrhenian Sea and the other inland; not shown). For the initial development stage of the cyclone (from 9 to 36 h after the start of simulation), the three configurations produce significant mean errors of 39, 44, and 64 km.

In contrast, the cyclones simulated with the other five microphysical schemes remain much closer to the observed track (Figures 4a and 5a). The small distance in Table 2 is also indicative of the good time accuracy of the simulations, WRFUNCL7 being the best run.

After landfall near Napoli, the MTLC moved inland and in this phase did not show tropical characteristics [6]. The second tropical transition occurred during its transit over the Adriatic Sea (Figure 1a), where first it moved northward and then south-southeastward. At this stage, several runs (WRFUNC2-4-6-7-8) describe accurately the track of the cyclone (Figure 5a). However, the final part of the cyclone is reproduced well only in WRFUNC7 (Figure 5a); in fact, the final and weakest stages in the cyclone lifetime are generally less predictable in terms of track and minimum pressure [15].

The time evolution of mean sea level pressure (MSLP) in Napoli (Figure 6a), Ortona (Figure 6b), and Ancona stations (Figure 6c) shows that the evolution of the cyclone was reproduced in all simulations, although the model responses could change by several hPa, in particular in Ortona, depending on the large spread of the cyclone track near the Adriatic coast. About the time evolution in wind speed in the same stations (Figure 7), the interpretation was less straightforward considering that the 10 m wind is sensitive to small variations in the cyclone track and pressure distribution.



**Figure 4.** Mediterranean tropical-like cyclone (MTLC) trajectories for the simulations using different microphysics (a) and planetary boundary layer (PBL) schemes (b).

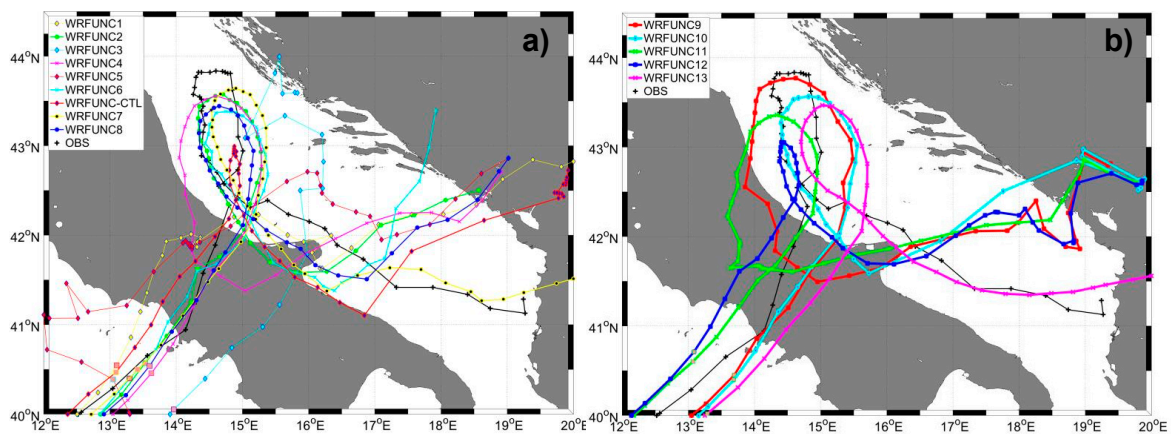


**Figure 5.** Zoom view of the cyclone trajectories in the simulations using different microphysics (a) and PBL schemes (b).



**Table 2.** Average value of geometric distance from the observed track in the whole track (top), in the first phase (middle) and along the Adriatic Sea (bottom).

<b>Pb11 Mp8 dt600</b>	<b>Pb11 Mp8 Dt1800</b>	<b>Pb11 Mp14 Dt600</b>	<b>Pb11 Mp14 Dt1800</b>	<b>Pb12 Mp8 Dt600</b>	<b>Pb12 Mp8 Dt1800</b>	<b>Pb12 Mp14 Dt600</b>	<b>Pb12 Mp14 Dt1800</b>	<b>Pb15 Mp8 Dt600</b>	<b>Pb15 Mp8 Dt1800</b>	<b>Pb15 Mp14 Dt600</b>	<b>Pb15 Mp14 Dt1800</b>	<b>Pb18 Mp8 Dt600</b>	<b>Pb18 Mp8 Dt1800</b>	<b>Pb18 Mp14 Dt600</b>	<b>Pb15 Mp14 Dt1800</b>
30.12	36.81	43.89	44.25	34.65	36.6	33.9	35.2	47.4	37.5	38.8	37.7	31.7	39.9	47.9	38.01
26.84	27.49	46.24	45	27	27.13	28.8	27.7	32.41	26.79	25.97	27.1	35.22	39.22	49.31	47.7
27.6	33.33	40.22	41.02	31.28	31	30.8	31.5	45	35.28	36.43	35.25	32	35.9	44.6	38.5
<b>Pb11 Mp8 dt600</b>	<b>Pb11 Mp8 Dt1800</b>	<b>Pb11 Mp14 Dt600</b>	<b>Pb11 Mp14 Dt1800</b>	<b>Pb12 Mp8 Dt600</b>	<b>Pb12 Mp8 Dt1800</b>	<b>Pb12 Mp14 Dt600</b>	<b>Pb12 Mp14 Dt1800</b>	<b>Pb15 Mp8 Dt600</b>	<b>Pb15 Mp8 Dt1800</b>	<b>Pb15 Mp14 Dt600</b>	<b>Pb15 Mp14 Dt1800</b>	<b>Pb18 Mp8 Dt600</b>	<b>Pb18 Mp8 Dt1800</b>	<b>Pb18 Mp14 Dt600</b>	<b>Pb15 Mp14 Dt1800</b>
30.12	36.81	43.89	44.25	34.65	36.6	33.9	35.2	47.4	37.5	38.8	37.7	31.7	39.9	47.9	38.01
26.84	27.49	46.24	45	27	27.13	28.8	27.7	32.41	26.79	25.97	27.1	35.22	39.22	49.31	47.7
27.6	33.33	40.22	41.02	31.28	31	30.8	31.5	45	35.28	36.43	35.25	32	35.9	44.6	38.5

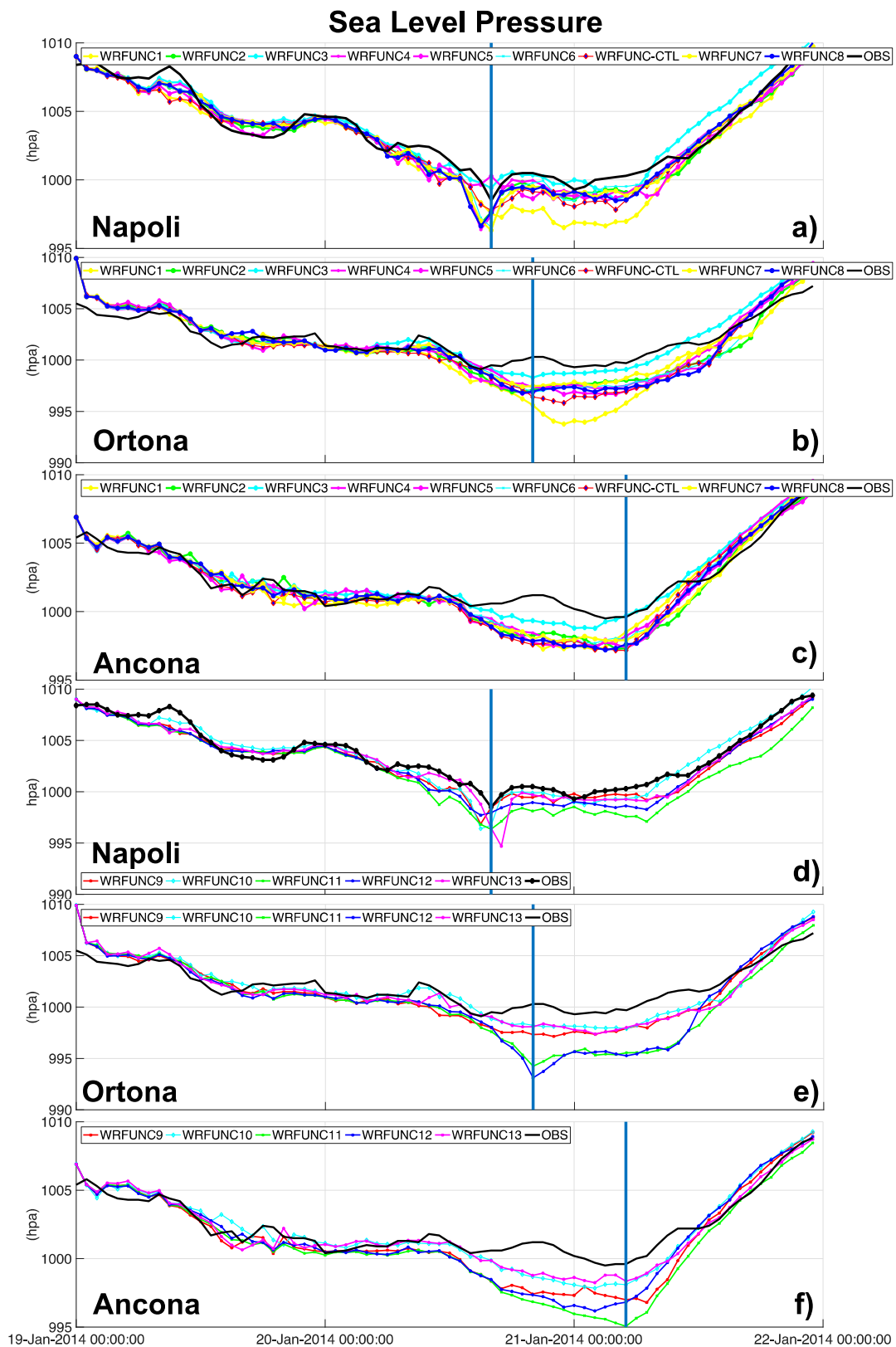


**Figure 6.** Comparison between the mean sea level pressure (MSLP) at Napoli, Ortona, and Ancona weather stations and the MSLP generated by numerical simulations. (a–c) data with different microphysics schemes; (d–f) data with PBL parameterizations. The blue lines indicate the landfall time over the Napoli station (a–d) and the time when the cyclone arrives close to the other stations, Ortona and Ancona.

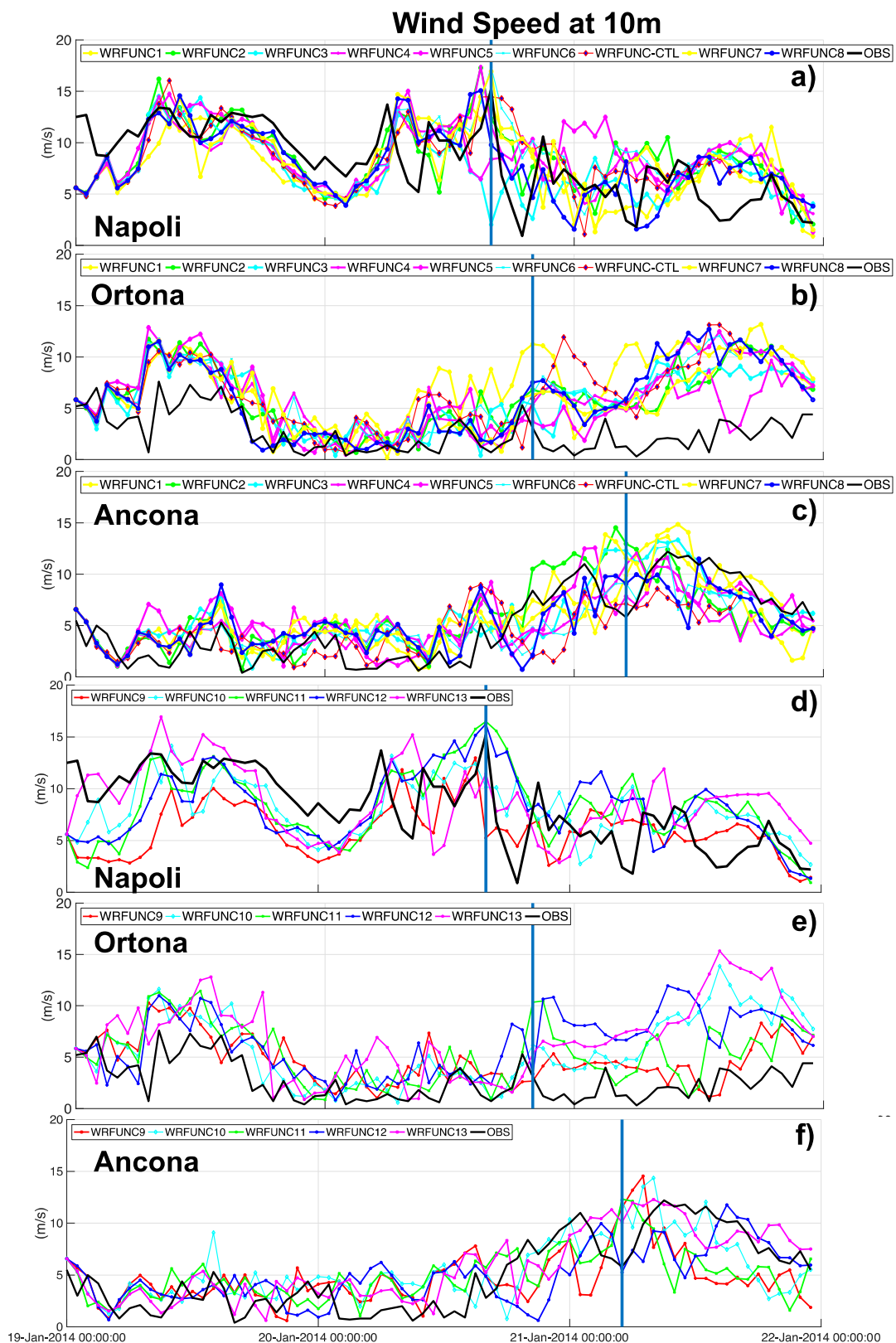


**Figure 7.** As in Figure 6 but for the wind speed for all uncoupled simulations. (a–c) data with different microphysics schemes; (d–f) data with PBL parameterizations. The blue lines indicate the landfall time over the Napoli station (a–d) and the time when the cyclone arrives close to the other stations, Ortona and Ancona.

The minimum pressure in the center of the cyclone and the maximum wind intensity nearby, calculated along the track, are shown in Figure 8. The simulated data are comparable with the observations in the points highlighted in blue, which represent respectively the surface station data near the Strait of Gibraltar and in Napoli. In general, the model simulations overestimate the pressure drop at the center of the cyclone by a few hPa, thus producing greater pressure gradients and overestimating the wind speed on average by some m/s, which is a known general problem of WRF model simulations [42].

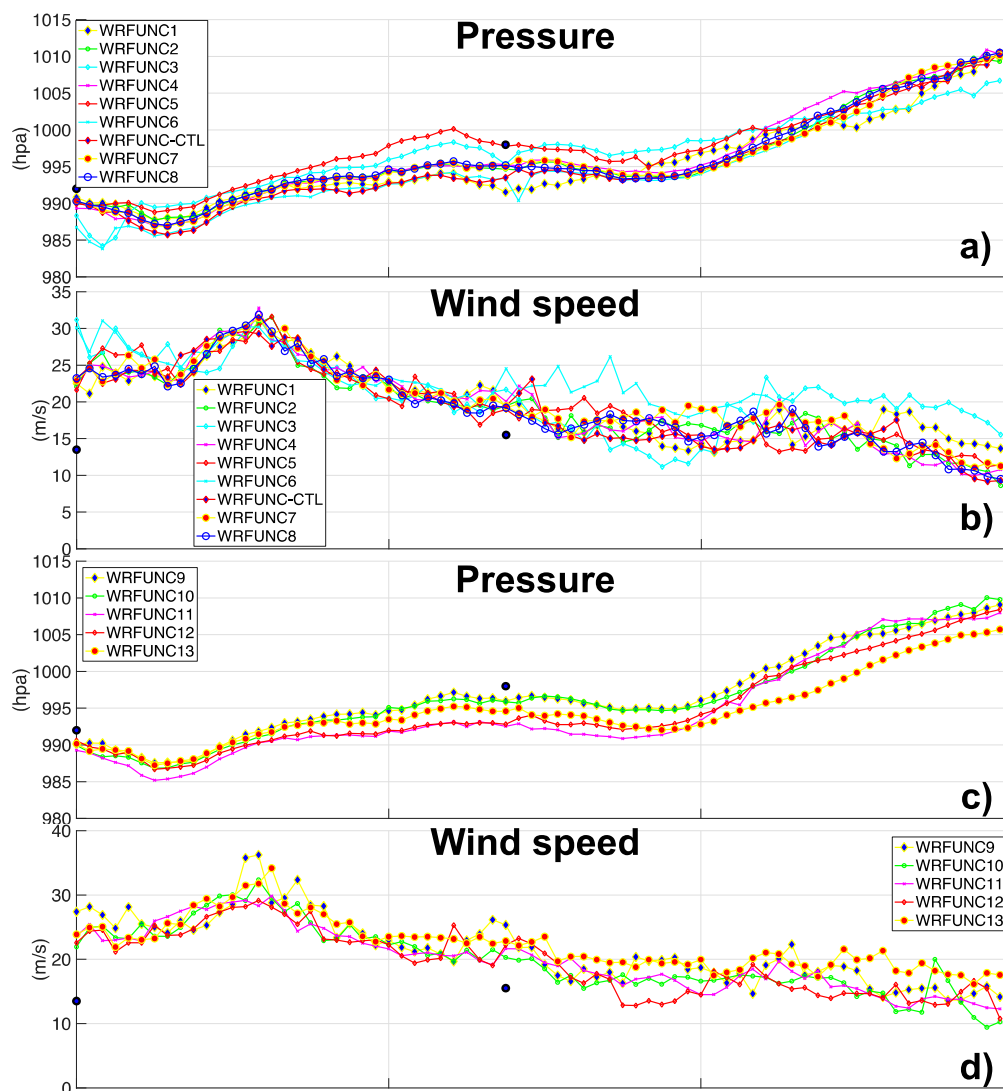


**Figure 8.** (Panels a,b) represent the MSLP and maximum wind speed in the cyclone center in *uncoupled* runs, (panels c,d) show the MSLP and wind speed comparison for *coupled* runs, in a radius of 200 km around the cyclone along the track. Blue dots represent the value in terms of MSLP and wind speed, respectively, in the early stage of cyclone and during the landfall in Napoli.

To summarize the results in this subsection, we analyzed several simulations performed with different microphysics. This sensitivity approach may give different results from case to case: for example, the MTLT studied in Miglietta et al., 2015, shows better performances with the [39] microphysics scheme (WRFUNC-CTL); on the other hand, [22], for their case suggest a weak sensitivity to the microphysics. In the present study, all microphysical schemes overestimate the intensity of the cyclone; however, the double-moment microphysical schemes (in particular, the WDM5 scheme with five classes of hydrometeors) seem to achieve better results when compared to single-moment

schemes. In particular, the run using the WDM5 microphysics better reproduces the circular path that the cyclone took over the Adriatic Sea, especially in the northern part of the track and along the North Adriatic coast, when the MTLC moved along an intense gradient of SSTs (see later). Finally, the use of different microphysical schemes affects the calculation time by about 30%, from the fastest scheme from Lin et al. to the most computational demanding WDM6 scheme.

### 3.2. PBL Schemes

Observing the trajectory followed by runs with different PBL schemes (Figure 4b), one can see that, in the first part of the event, when the MTLC moves over the western Mediterranean sea, the differences among the simulated paths and the observed trajectory increase with the time spent over the sea (as in [22]). This suggests that the interaction between the PBL and the sea surface needs some time to settle before influencing higher levels; in fact, in this tropical-like cyclone (TLC) phase (from 1 to 36 h), all simulations show a similar path with geometric distances from the observed track ranging on average between 26 and 30 km. However, before landfall the WRFUNC11 (QNSE scheme, [43]) and the WRFUNC12 runs (MYNN2 scheme, [44]) generate a northward shift of about 110 and 150 km, compare to observations.

In the second phase of the MTLC (from the 36th to the 70th h), over the Adriatic Sea, the track in the WRFUNC11 run remains west of the other runs, closer to the Adriatic coast of Italy, where it makes a second (erroneous) landfall at latitude 43° N. Similarly, the WRFUNC9 produces a wide trajectory along the Adriatic, keeping close to the observed track, but it still makes an erroneous landfall over the Adriatic coast of Italy. The shape of the track in WRFUNC10 and WRFUNC13 simulations remains very close to the observed trajectory, as both produce a circle over the sea similar to the observed trajectory. In the final part of the trajectory, the BouLac scheme (WRFUNC13) represents the path of the cyclone much better, with a smaller geometrical distance (around 31 km). However, this is not considered as the “reference” PBL scheme because, in this phase, the depression is weaker and does not show the tropical features we are interested in.

The simulations WRFUNC10 and WRFUNC13 also show a more realistic intensity in the two Adriatic stations (Ancona and Ortona), with a bias of about 2 hPa compared to the other schemes, which overestimate the cyclone depth by about 5 hPa (Figure 6). Similar results are obtained in the timeseries in Figure 8, where the WRFUNC11 and WRFUNC12 runs overestimate the pressure depth by several hPa.

As shown in [45], the physical processes in the PBL drive energy exchanges at the interface with the sea, and these exchanges influence the evolution of the atmospheric phenomena at a synoptic level. Not surprisingly, we found a strong sensitivity to PBL schemes: as for the microphysics, the PBL schemes that develop a northward-shift in the trajectories move the cyclone closer to the Adriatic coast, so that it loses energy earlier due to landfall, and weakens in the Italian hinterland. As a consequence, as shown in Figure 6, the intensity of the cyclone diverges among the various runs more significantly after landfall. Finally, the PBL scheme marginally influences the computational times. For example the MYJ scheme (WRFUNC10) is 8% slower than other parameterizations.

### 3.3. Role of SST and Coupled Simulation

During the genesis of the MTLC, the western Mediterranean Sea shows an average positive SST anomaly of around 0.2 °C, compared to climatology data from 1980 to 2010 (from GOS-CNR Rome); however, in the Adriatic Sea, the anomaly is up to 1.8 °C (Figure 2). The large difference in SST between these two basins and the strong gradient of SST in the Adriatic Sea, in particular near the Italian coast, in the same area where the TLC intensifies (see Figure 1a) suggested that the effect of SST on the dynamics of this event should be investigated. In the first part of the TLC path, the simulation WRFUNC14 (an OML with an MLD of 80 m over the entire basin) reproduces a trajectory close to the observed path, with an average geometrical distance of 28 km, and a higher accuracy in the first stage (25 km) compared to the second stage (30 km).

Compared to the WRFUNC10 run (an OML with an MLD of 50 m), the track in the WRFUNC14 simulation (an MLD of 80 m) is very close (Figure 9), while some discrepancies occur in the pressure minimum, which is about 2 hPa deeper (and farther from the observations) at landfall near Napoli (Figure 10a). This is probably caused by the stronger heat fluxes and greater energy available for convection, due to the deeper mixed layer (Figure 11c). Overall, during the transit of the cyclone over the Adriatic Sea, the differences with respect to WRFUNC10 appear small (Figures 9–11).

The run WRFUNC15 uses a uniform SST of approximately 16.6 °C in the whole domain (average value encountered by the cyclone along its track). The trajectory of this run is comparable with those produced by the other simulations in the first stage of the TLC, with the landfall shifted southward by about 30 km and with an average distance from the observed track of 42 km in the first stage and 60 km in the second, respectively. In the second part, the track is shifted to the east and describes a narrower circle (Figure 9). The intensity of the storm is comparable with the other simulations during the first 15–18 h; however, after moving for about 10 h over the Mediterranean Sea, the cyclone rapidly intensifies, becoming 4 hPa deeper than the other runs (Figures 10a and 11a). During the transit over the Adriatic Sea, the cyclone does not weaken, differently from the other simulations, and the pressure minimum becomes 13 hPa deeper at the end of the simulation (Figure 11a). This is due to the fact that the Adriatic Sea is colder than the Tyrrhenian Sea; thus, in WRFUNC15 the temperature is higher than the real value, and fluxes are more intense (Figure 11c).

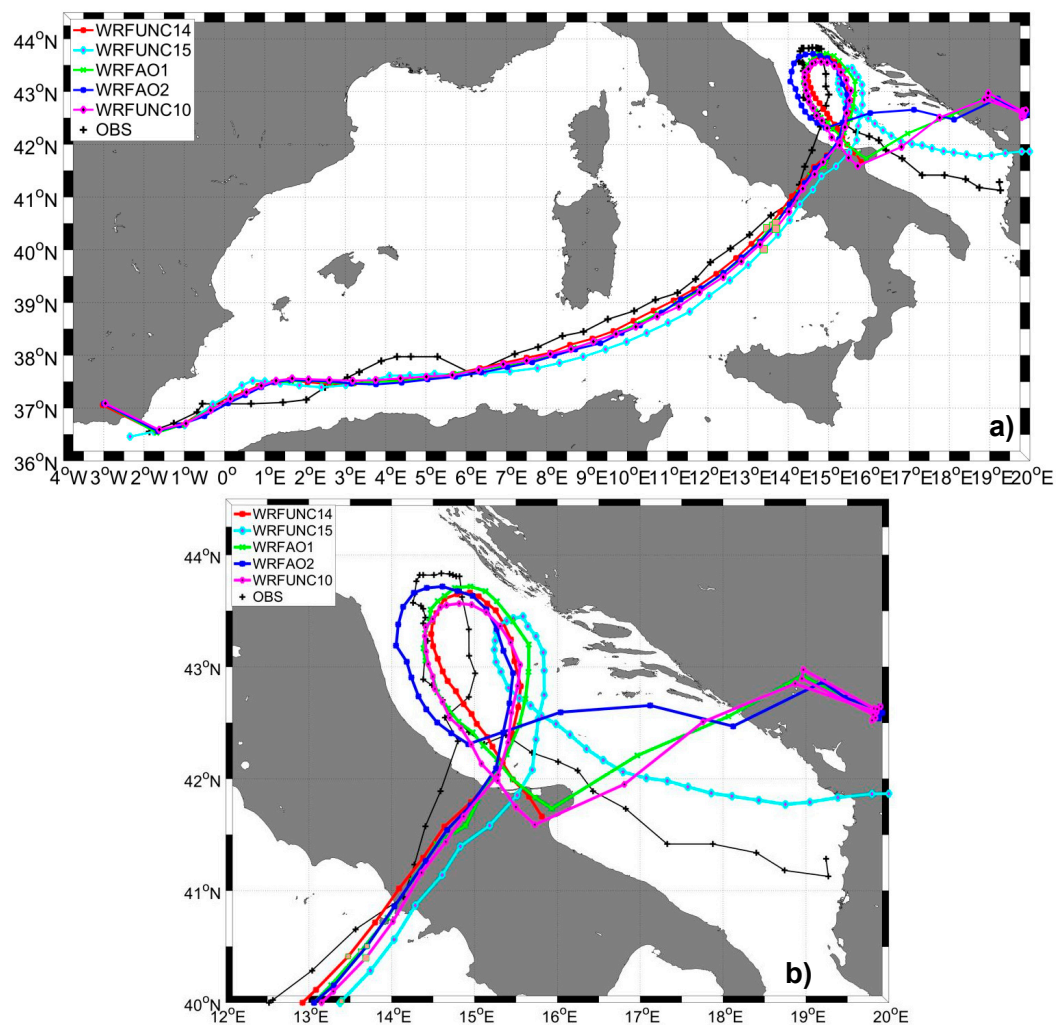


**Figure 9.** MTL simulated trajectories over the full domain (a) and zoom over the last part of the track (b) in the simulations WRFUNC14–15, AO1, AO2, and, for the sake of comparison, WRFUNC10.

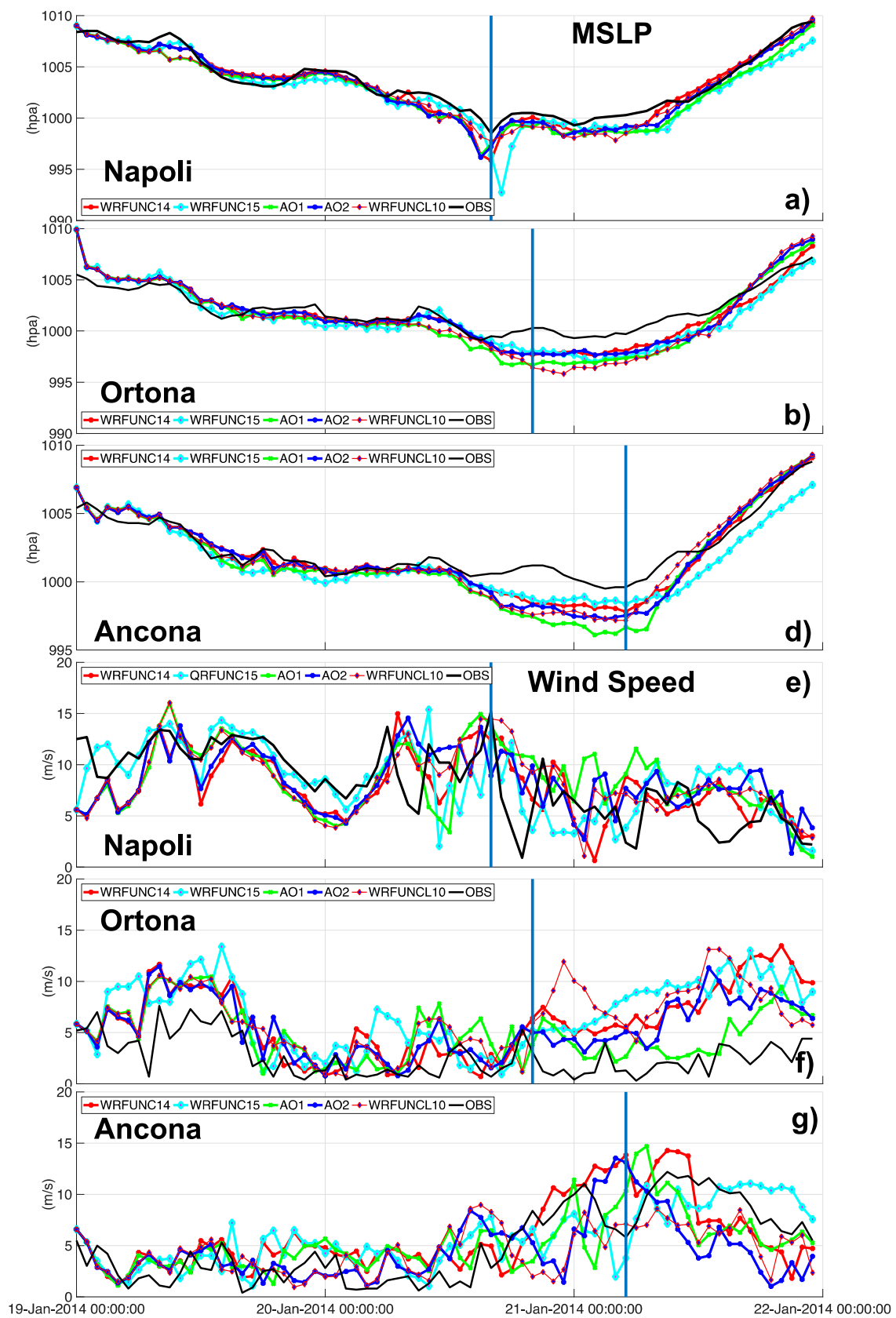


**Figure 10.** Observed and simulated MSLP (a–c) and wind speed (e–g) in Napoli, Ortona, and Ancona weather stations (WRFUNC10–14–15, AO1, and AO2 runs). The blue lines indicate the landfall time near the Napoli station (a–d) and the time when the cyclone arrives near the other stations, Ortona and Ancona.

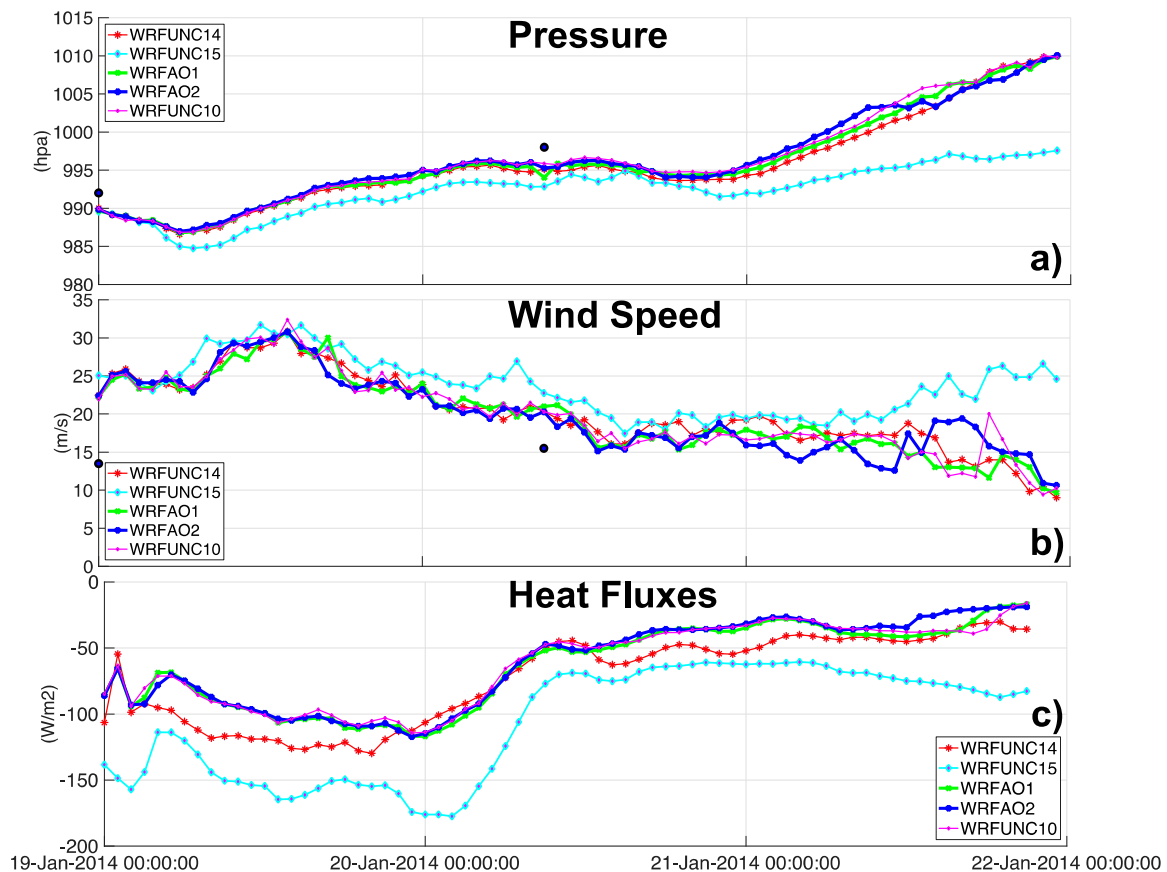


**Figure 11.** MSLP in the cyclone center (panel a) and maximum wind speed (panel b) and heat fluxes (panel c) in a radius of 200 km around the cyclone. Blue dots represent the MSLP and wind speed observed in the early stage of cyclone and during the landfall in Napoli, respectively. In panel (c), the mean heat fluxes over the same area (with a radius of 200 km around the center) are shown.

The trajectories of the atmosphere–ocean coupled runs AO1 and AO2 are shown in Figure 9. The run AO1 is characterized by an exchange time interval of 1800 s. This simulation generates the trajectory closest to that observed (Figure 9) among all runs (coupled and uncoupled). The distance between the estimated and simulated trajectory remains small for the entire cyclone lifetime, apart from the last stage (Figure 9 and Table 2). Additionally, the landfall takes place a few kilometers away from the observed location (Figure 9). Temporal evolution and intensity are also consistent with measurements, apart from a small overestimation of the cyclone intensity (Figure 10). Along the cyclone track, the minimum pressure is about 2 hPa deeper than the two available observations (Figure 11a), while the wind intensity near the cyclone center is slightly overestimated.

The AO2 coupled simulation uses an exchange time interval of 600 s. Its track is very similar to the AO1 run, in particular in the first phase, while later it moves closer to the Adriatic coast of Italy (Figure 9); additionally, AO2 better reproduces the intensity of the cyclone near the Italian Adriatic coast. In the latter phase, in the morning of January 21, the cyclone weakens before moving very rapidly towards the east. This weakening is probably caused by the passage of the simulated cyclone over very cold coastal waters (Figure 1), which decrease the intensity of the sea surface fluxes that feed the system (Figure 11c).



Greater sea surface fluxes, like those simulated in WRFUNC14 and WRFUNC15, provide more energy to the cyclone. However, they do not affect its intensity immediately; they require a time period during which the cumulative effects of air–sea interaction processes become effective (as in Figure 4 in [9]). For example, as shown in Figure 11c, while the WRFUNC15 simulation generates more intense heat fluxes than the other runs over the whole simulation length, the difference in terms of wind and pressure fields increases significantly only near the end of the runs.

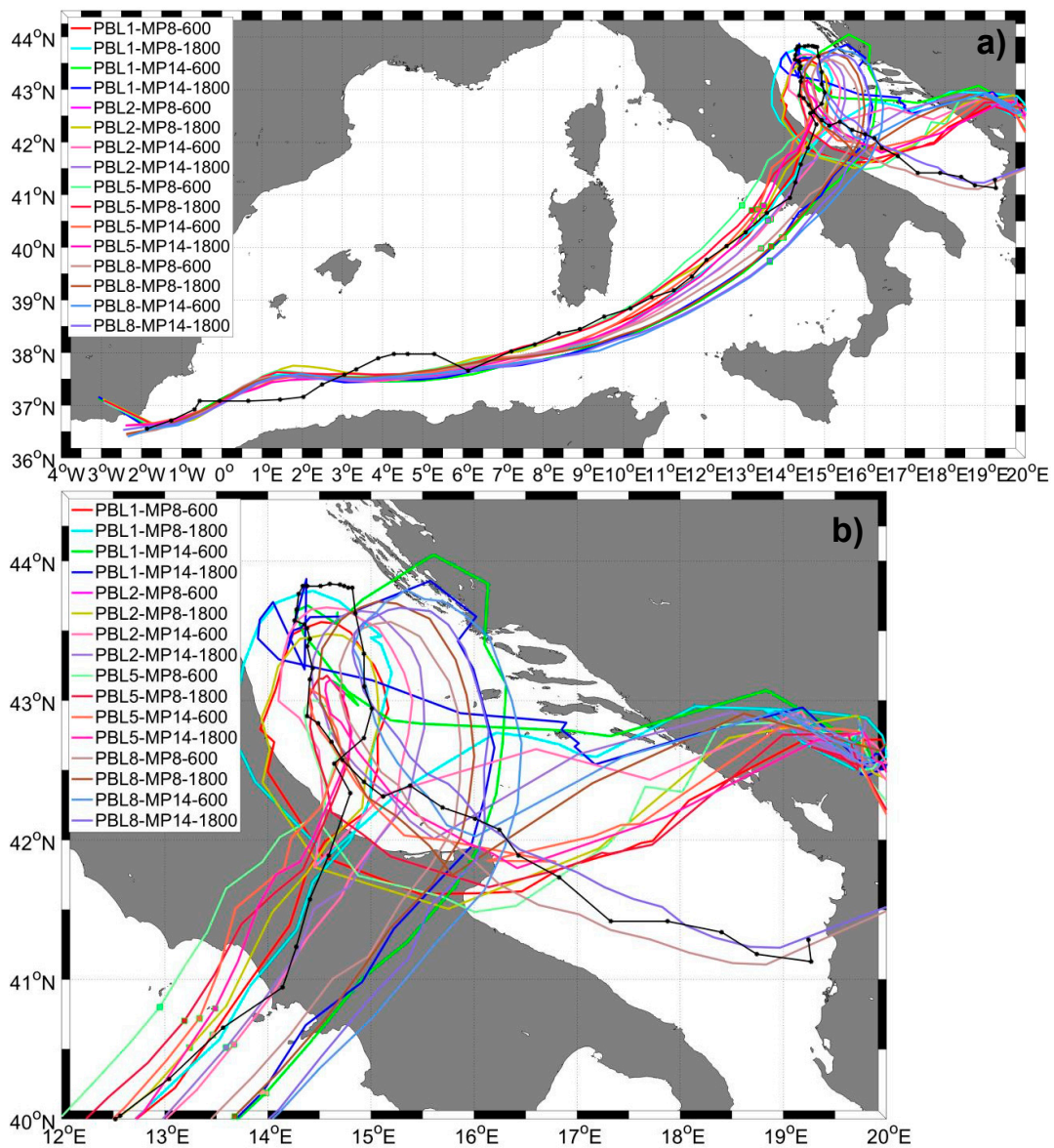
The sensitivity to SST and the analysis of the coupled simulations suggest some relevant indications for hindcast and forecast applications. We found that the use of the 1D OML model, when it starts from a high-resolution SST field similar to that employed in the initial conditions of the coupled runs, allows for an overall good estimate of the physical and dynamical characteristics of the cyclone, although the depth of the OML affects the results. The latter point is apparent in particular in the Adriatic Sea, which is a semi-enclosed basin with a complex oceanic circulation and intense horizontal thermal gradients of SST [46].

#### 3.4. Sensitivity Analysis of the Coupled Simulations

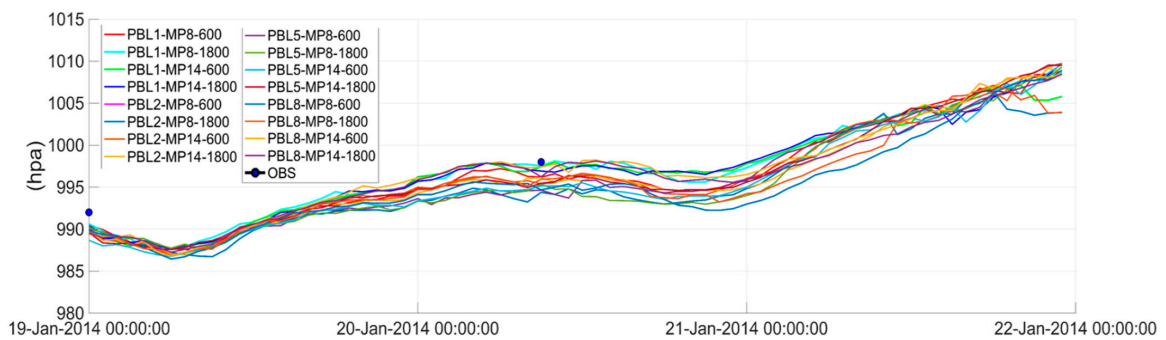
The goal of the present section is to disentangle the effect of coupling, that of the parameterization schemes, and that of the coupling exchange time on the simulation of the MTLC. We consider a set of coupled model simulations, differing between oceanic and atmospheric models in terms of the PBL, microphysics, and communication time (DT). For the PBL, we used YSU (Yonsei University), MYJ (Mellor-Yamada-Janjic), MYNN (Mellor-Yamada-Nakanishi-Niino), and BouLac (Bougeault-Lacarrère), already considered in the uncoupled runs. For the microphysics, we focused on the two schemes that are computationally more efficient, i.e., WDM5 (WRF double moment five-class microphysics) and the [39] scheme. The chosen integration timesteps are 1800 s (consistent with the approach previously adopted in the coupled runs) and 600 s.

Table 2 shows how the geometrical distance varies among the simulations. The change in the microphysics (MP8 and MP14) is responsible for significant variations, especially in the case of PBL1 (Figure 12). In fact, for PBL1 runs, while MP8 produces trajectories, landfalls, and time evolutions very close to the observed data, the use of MP14 shifts the landfall to the south by almost 40 km (Figure 12). In contrast, the effect of communication time for PBL1 runs is small. For PBL2, the simulated tracks are all close to the observed trajectory, and the effects of microphysics and coupling time are minor (Table 2). Lastly, the use of PBL5 or PBL8 schemes causes a shift in the trajectories, respectively, to the north (PBL5) and to the south (PBL8) by approximately 100 km, which is compared to the observed track (Figure 12): in these cases, the communication time has a significant effect on the model track, especially in the second part of the simulations.

After the landfall in Napoli, one may note a rapidly growing divergence among the trajectories (Figure 12b): the PBL1 and PBL2 schemes produce tracks closer to the observed one, PBL5 generates trajectories shifted toward the Italian Adriatic coast and a slower evolution, and PBL8 generates trajectories shifted to the east. Figure 13 shows a spread of almost 5 hPa among the runs in the phase of the maximum strength of the cyclone. The simulations using the schemes PBL1 and PBL2 show the best results with a difference from observations of only 1 hPa. The choice of the timing of communication slightly affects the development of the MTLC, which is slightly more intense for the smallest exchange time.



**Figure 12.** MTLC simulated trajectories over the full domain (a) and zoom of trajectories over the last part of the track (b) in the coupled simulations that use a different PBL, a different microphysics scheme, and a different coupling time.



**Figure 13.** Minimum MSLP versus time. Blue dots represent the MSLP in the early stage of cyclone and during the landfall in Napoli.

#### 4. Conclusions and Remarks

In this work, we investigate in detail the impact of different factors that drive the air–sea interaction during the numerical simulation of an MTLC. After a stand-alone atmospheric model approach, the COAWST coupled modeling system was used, varying microphysics and planetary boundary layer schemes and implementing the coupling between atmospheric and oceanic models with different exchange times. The role of SST was also studied in the uncoupled simulations considering two different OML depths (50 and 80 m) in a slab ocean model and imposing a uniform SST field over all the ocean grid points.

The main findings emerging from the simulations can be summarized as follows:

- a sensitivity to the microphysics and boundary layer schemes was observed, which may significantly affect the track, even more than the intensity, of the cyclone;
- the sensitivity to coupling time is limited compared to do that to physics parameterizations and is dependent on the set of schemes considered;
- the 1D ocean model, although it suffers from limited flexibility (MLD set in the model namelist), is able to reproduce pretty well the evolution of the cyclone, given a high-resolution initial SST field produced by ROMS after a long spin-up time;
- air–sea interaction processes are fundamental for the proper numerical simulation of the cyclone, and substituting the real SST with an average field may dramatically affect the intensity of the cyclone;
- atmosphere–ocean coupled systems are the best way to take into account realistically and in a consistent way the exchange of heat and momentum between the atmosphere and the ocean.

We can now return to the original question we posed at the beginning of the paper, i.e., whether a multi-physics ensemble or a coupled atmosphere–ocean modeling system is ideal for simulating Mediterranean cyclones, and from the perspective of operational use. Our conclusions are the following:

- A multi-physics ensemble, using different PBL and microphysical parameterization schemes, produces a large spread, especially in terms of cyclone track.
- The spread of a multi-physics ensemble is too large to provide any useful information about the detailed areas possibly affected by the cyclone, and this is probably a consequence of the fact that some physical schemes are not specifically tuned for the Mediterranean area.
- A comprehensive study, including a large number of cases of Mediterranean cyclones, should be performed, in order to identify the parameterization(s) that perform better in the region for these specific features; in search of the best configuration, one probably will not find that a certain numerical setup is the best for all cases (Pytharoulis et al., 2018), but it is plausible that a few implementations will work reasonably well for all cyclones.
- After an “optimal” setup is identified, a coupled numerical simulation after a long spin up time should provide a high-resolution SST field as a lower boundary to the atmospheric model.
- If the computational resources are sufficient, a coupled numerical simulation should be performed, since only this strategy allows one to correctly reproduce the exchange of heat and momentum between the ocean and the atmosphere. Although the advantage in terms of cyclone track and intensity is limited in the present case, we reasonably expect that a great benefit in terms of the operational prediction of wind speed, surface fluxes, and precipitation (Ricchi et al., 2016) can be achieved.

**Author Contributions:** Conceptualization, A.R., G.C. and S.C.; Methodology, A.R.; Software, A.R.; Validation, A.R., D.B., M.M.M., G.C., U.R. and S.C.; Formal Analysis, A.R., D.B., M.M.M., G.C., U.R. and S.C.; Investigation, A.R., D.B., M.M.M., G.C., U.R. and S.C.; Resources, A.R.; Data Curation, A.R., D.B., M.M.M., G.C., U.R. and S.C.; Writing–Original Draft Preparation, A.R., D.B., M.M.M. and S.C.; Writing–Review & Editing, A.R., D.B., M.M.M., G.C., U.R. and S.C.; Visualization, A.R., D.B.; Supervision, A.R. and S.C.; Project Administration, S.C.; Funding Acquisition, S.C.

**Funding:** This work was supported by RITMARE National Flagship initiative funded by the Italian Ministry of Education, University and Research (IV Phase, Line 5, “Coastal Erosion and Vulnerability”) and by the EU H2020 Programme (CEASELESS Project, grant agreement No. 730030).

**Acknowledgments:** Authors acknowledge the CINECA award under the ISCRA initiative (grant HP10C2SECI “COMOLF”, Coupled Regional Modeling in Coastal Oceans, P.I. Antonio Ricchi) and specifically the kind assistance of Isabella Baccarelli. The work was partially supported by the EU contract 730030 (call H2020-EO-2016, “CEASELESS”, Coordinator A. Arcilla) and by RITMARE national flagship initiative funded by the Italian Ministry of University and Research (IV phase, Line 5, “Coastal Erosion and Vulnerability”, P.I. Sandro Carniel).

**Conflicts of Interest:** The authors declare no conflict of interest.

## References

1. Campins, J.; Genovés, A.; Picornell, M.A.; Jansà, A. Climatology of Mediterranean cyclones using the ERA-40 dataset. *Int. J. Climatol.* **2010**, *31*, 1596–1614. [[CrossRef](#)]
2. Buzzi, A.; Tibaldi, S. Cyclogenesis in the lee of the Alps: A case study. *Q. J. R. Meteorol. Soc.* **1978**, *104*, 271–287. [[CrossRef](#)]
3. Rasmussen, E.; Zick, C. A subsynoptic vortex over the Mediterranean with some resemblance to polar lows. *Tellus A* **1987**, *39A*, 408–425. [[CrossRef](#)]
4. Lagouvardos, K.; Kotroni, V.; Nickovic, S.; Jovic, D.; Kallos, G.; Tremback, C.J. Observations and model simulations of a winter sub-synoptic vortex over the central Mediterranean. *Meteorol. Appl.* **1999**, *6*, 371–383. [[CrossRef](#)]
5. Royal Meteorological Society (Great Britain). In *Meteorological Applications*; Cambridge University Press: Cambridge, UK, 2000.
6. Cioni, G.; Malguzzi, P.; Buzzi, A. Thermal structure and dynamical precursor of a Mediterranean tropical-like cyclone. *Q. J. R. Meteorol. Soc.* **2016**, *142*, 1757–1766. [[CrossRef](#)]
7. Tous, M.; Romero, R.; Ramis, C. Surface heat fluxes influence on medicane trajectories and intensification. *Atmos. Res.* **2013**, *123*, 400–411. [[CrossRef](#)]
8. Miglietta, M.M.; Laviola, S.; Malvaldi, A.; Conte, D.; Levizzani, V.; Price, C. Analysis of tropical-like cyclones over the Mediterranean Sea through a combined modelling and satellite approach. *Geophys. Res. Lett.* **2013**, *40*, 2400–2405. [[CrossRef](#)]
9. Miglietta, M.M.; Rotunno, R. Development Mechanisms for Mediterranean Tropical-Like Cyclones (Medicanes). *Q. J. R. Meteorol. Soc.* **2019**. [[CrossRef](#)]
10. Emanuel, K. Increasing destructiveness of tropical cyclones over the past 30 years. *Nature* **2005**. [[CrossRef](#)]
11. Cavicchia, L.; von Storch, H.; Gualdi, S. Mediterranean Tropical-Like Cyclones in Present and Future Climate. *J. Clim.* **2014**, *27*, 7493–7501. [[CrossRef](#)]
12. Miglietta, M.M.; Cerrai, D.; Laviola, S.; Cattani, E.; Levizzani, V. Potential vorticity patterns in Mediterranean “hurricanes”. *Geophys. Res. Lett.* **2017**, *44*, 2537–2545. [[CrossRef](#)]
13. Di Muzio, E.; Riemer, M.; Fink, A.H.; Maier-Gerber, M. Assessing the predictability of Medicanes in ECMWF ensemble forecasts using an object-based approach. *Q. J. R. Meteorol. Soc.* **2019**. [[CrossRef](#)]
14. Cioni, G.; Cerrai, D.; Klocke, D. Investigating the predictability of a Mediterranean tropical-like cyclone using a storm-resolving model. *Q. J. R. Meteorol. Soc.* **2018**, *144*, 1598–1610. [[CrossRef](#)]
15. Miglietta, M.M.; Mastrangelo, D.; Conte, D. Influence of physics parameterization schemes on the simulation of a tropical-like cyclone in the Mediterranean Sea. *Atmos. Res.* **2015**, *153*, 360–375. [[CrossRef](#)]
16. Ragone, F.; Mariotti, M.; Parodi, A.; Von Hardenberg, J.; Pasquero, C. A Climatological Study of Western Mediterranean Medicanes in Numerical Simulations with Explicit and Parameterized Convection. *Atmosphere* **2018**, *9*, 397. [[CrossRef](#)]
17. Pytharoulis, I.; Kartsios, S.; Tegoulas, I.; Feidas, H.; Miglietta, M.; Matsangouras, I.; Karacostas, T. Sensitivity of a Mediterranean Tropical-Like Cyclone to Physical Parameterizations. *Atmosphere* **2018**, *9*, 436. [[CrossRef](#)]
18. Davolio, S.; Miglietta, M.M.; Moscatello, A.; Pacifico, F.; Buzzi, A.; Rotunno, R. Natural Hazards and Earth System Sciences Numerical forecast and analysis of a tropical-like cyclone in the Ionian Sea. *Hazards Earth Syst. Sci.* **2009**, *9*, 551–562. [[CrossRef](#)]
19. Miglietta, M.M.; Moscatello, A.; Conte, D.; Mannarini, G.; Lacorata, G.; Rotunno, R. Numerical analysis of a Mediterranean ‘hurricane’ over south-eastern Italy: Sensitivity experiments to sea surface temperature. *Atmos. Res.* **2011**, *101*, 412–426. [[CrossRef](#)]

20. Pytharoulis, I.; Matsangouras, I.T.; Tegoulis, I.; Kotsopoulos, S.; Karacostas, T.S.; Nastos, P.T. *Prospectives on Atmospheric Sciences*; Springer: Cham, Switzerland, 2017; pp. 115–121. [[CrossRef](#)]
21. Akhtar, N.; Brauch, J.; Dobler, A.; Béranger, K.; Ahrens, B. Medicanes in an ocean-atmosphere coupled regional climate model. *Hazards Earth Syst. Sci.* **2014**, *14*, 2189–2201. [[CrossRef](#)]
22. Ricchi, A.; Miglietta, M.; Barbariol, F.; Benetazzo, A.; Bergamasco, A.; Bonaldo, D.; Cassardo, C.; Falcieri, F.M.; Modugno, G.; Russo, A.; et al. Sensitivity of a Mediterranean Tropical-Like Cyclone to Different Model Configurations and Coupling Strategies. *Atmosphere* **2017**, *8*, 92. [[CrossRef](#)]
23. Warner, J.C.; Armstrong, B.; He, R.; Zambon, J.B. Development of a Coupled Ocean—Atmosphere—Wave—Sediment Transport (COAWST) Modeling System. *Ocean Model.* **2010**, *35*, 230–244. [[CrossRef](#)]
24. Warner, J.C.; Sherwood, C.R.; Signell, R.P.; Harris, C.K.; Arango, H.G. Development of a three-dimensional, regional, coupled wave, current, and sediment-transport model. *Comput. Geosci.* **2008**, *34*, 1284–1306. [[CrossRef](#)]
25. Ricchi, A.; Miglietta, M.M.; Falco, P.P.; Benetazzo, A.; Bonaldo, D.; Bergamasco, A.; Sclavo, M.; Carniel, S. On the use of a coupled ocean–atmosphere–wave model during an extreme cold air outbreak over the Adriatic Sea. *Atmos. Res.* **2016**, *172–173*, 48–65. [[CrossRef](#)]
26. Olabarrieta, M.; Warner, J.C.; Armstrong, B.; Zambon, J.B.; He, R. Ocean–atmosphere dynamics during Hurricane Ida and Nor’Ida: An application of the coupled ocean–atmosphere–wave–sediment transport (COAWST) modeling system. *Ocean Model.* **2012**, *43–44*, 112–137. [[CrossRef](#)]
27. Skamarock, W.C. Coauthors, 2008: A description of the Advanced Research WRF version 3. NCAR Tech. Note NCAR/TN-475+STR. p. 113. Available online: <https://doi.org/10.5065/D68S4MVH> (accessed on 10 October 2018).
28. Shchepetkin, A.F.; McWilliams, J.C. The regional oceanic modeling system (ROMS): A split-explicit, free-surface, topography-following-coordinate oceanic model. *Ocean Model.* **2005**, *9*, 347–404. [[CrossRef](#)]
29. Warner, J.C.; Sullivan, C.; Voulgaris, G.; Work, P.; Haas, K.; Hanes, D.M. The South Carolina Coastal Erosion Study: Numerical Modeling of Circulation and Sediment Transport in Long Bay, SC. *Am. Geophys. Union, Fall Meet. 2004, Abstr. id. OS21B-1226*. Available online: <http://adsabs.harvard.edu/abs/2004AGUFMOS21B1226W> (accessed on 5 October 2018).
30. Larson, J.W.; Craig, A.P.; Drake, J.B.; Erickson, D.J.; Branstetter, M.L.; Ham, M.W. A Massively Parallel Dynamical Core for Continental-to Global-Scale River Transport. Available online: <http://people.physics.anu.edu.au/~{jw1105/Pubs/2007/larson-et-al-ParRTM-ModSim07.pdf> (accessed on 25 September 2018).
31. Jacob, R.; Larson, J.; Ong, E.  $M \times N$  Communication and Parallel Interpolation in Community Climate System Model Version 3 Using the Model Coupling Toolkit. *Int. J. High Perform. Comput. Appl.* **2005**, *19*, 293–307. [[CrossRef](#)]
32. Lim, K.-S.S.; Hong, S.-Y.; Lim, K.-S.S.; Hong, S.-Y. Development of an Effective Double-Moment Cloud Microphysics Scheme with Prognostic Cloud Condensation Nuclei (CCN) for Weather and Climate Models. *Mon. Weather Rev.* **2010**, *138*, 1587–1612. [[CrossRef](#)]
33. Janjić, Z.I. The Step-Mountain Eta Coordinate Model: Further Developments of the Convection, Viscous Sublayer, and Turbulence Closure Schemes. *Mon. Weather Rev.* **1994**, *122*, 927–945. [[CrossRef](#)]
34. Iacono, M.J.; Delamere, J.S.; Mlawer, E.J.; Shephard, M.W.; Clough, S.A.; Collins, W.D. Radiative forcing by long-lived greenhouse gases: Calculations with the AER radiative transfer models. *J. Geophys. Res.* **2008**, *113*, D13103. [[CrossRef](#)]
35. Dudhia, J.; Dudhia, J. Numerical Study of Convection Observed during the Winter Monsoon Experiment Using a Mesoscale Two-Dimensional Model. *J. Atmos. Sci.* **1989**, *46*, 3077–3107. [[CrossRef](#)]
36. Pinardi, N.; Allen, I.; Demirov, E.; De Mey, P.; Korres, G.; Lascaratos, A.; Le Traon, P.-Y.; Maillard, C.; Manzella, G.; Tziavos, C. The Mediterranean ocean forecasting system: First phase of implementation (1998–2001). *Ann. Geophys.* **2003**, *21*, 3–20. [[CrossRef](#)]
37. Sandwell, D.T. A detailed view of the South Pacific geoid from satellite altimetry. *J. Geophys. Res. Solid Earth* **1984**, *89*, 1089–1104. [[CrossRef](#)]
38. Warner, J.C.; Sherwood, C.R.; Arango, H.G.; Signell, R.P. Performance of four turbulence closure models implemented using a generic length scale method. *Ocean Model.* **2005**, *8*, 81–113. [[CrossRef](#)]
39. Thompson, G.; Field, P.R.; Rasmussen, R.M.; Hall, W.D. Explicit Forecasts of Winter Precipitation Using an Improved Bulk Microphysics Scheme. Part II: Implementation of a New Snow Parameterization. *Mon. Weather Rev.* **2008**, *136*, 5095–5115. [[CrossRef](#)]

40. Janjic, Z.I.; Gerrity, J.P., Jr.; Nickovic, S. An Alternative Approach to Nonhydrostatic Modeling. *Mon. Weather Rev.* **2008**, *129*, 1164–1178. [[CrossRef](#)]
41. Pollard, R.T.; Rhines, P.B.; Thompson, R.O.R.Y. The deepening of the wind-Mixed layer. *Geophys. Fluid Dyn.* **1972**, *4*, 381–404. [[CrossRef](#)]
42. Tateo, A.; Miglietta, M.M.; Fedele, F.; Menegotto, M.; Monaco, A.; Bellotti, R. Ensemble using different Planetary Boundary Layer schemes in WRF model for wind speed and direction prediction over Apulia region. *Adv. Sci. Res.* **2017**, *14*, 95–102. [[CrossRef](#)]
43. Sukoriansky, S.; Galperin, B.; Perov, V. A quasi-normal scale elimination model of turbulence and its application to stably stratified flows. *Nonlinear Process. Geophys.* **2006**, *13*, 9–22. [[CrossRef](#)]
44. Nakanishi, M.; Niino, H. An Improved Mellor–Yamada Level-3 Model: Its Numerical Stability and Application to a Regional Prediction of Advection Fog. *Boundary-Layer Meteorol.* **2006**, *119*, 397–407. [[CrossRef](#)]
45. Sukoriansky, S.; Galperin, B.; Staroselsky, I. A quasinormal scale elimination model of turbulent flows with stable stratification. *Phys. Fluids* **2005**, *17*, 085107. [[CrossRef](#)]
46. Carniel, S.; Benetazzo, A.; Bonaldo, D.; Falcieri, F.M.; Miglietta, M.M.; Ricchi, A.; Sclavo, M. Scratching beneath the surface while coupling atmosphere, ocean and waves: Analysis of a dense water formation event. *Ocean Model.* **2016**, *101*, 101–112. [[CrossRef](#)]



© 2019 by the authors. Licensee MDPI, Basel, Switzerland. This article is an open access article distributed under the terms and conditions of the Creative Commons Attribution (CC BY) license (<http://creativecommons.org/licenses/by/4.0/>).